Stick-slip nanofriction in trapped cold ion chains

D. Mandelli,[1] A. Vanossi,[1,2] and E. Tosatti[1,2,3]

[1]*International School for Advanced Studies (SISSA), Via Bonomea 265, 34136 Trieste, Italy*

[2]*CNR-IOM Democritos National Simulation Center, Via Bonomea 265, 34136 Trieste, Italy*

[3]*International Centre for Theoretical Physics (ICTP), Strada Costiera 11, 34014 Trieste, Italy*

(Received 24 March 2013; revised manuscript received 1 May 2013; published 10 May 2013)

Stick slip—the sequence of mechanical instabilities through which a slider advances on a solid substrate—is pervasive throughout sliding friction, from nanoscales to geological scales. Here we suggest that trapped cold ions in an optical lattice can also be of help in understanding stick-slip friction, and also the way friction changes when one of the sliders undergoes structural transitions. For that scope, we simulated the dynamical properties of a 101-ion chain, driven to slide back and forth by a slowly oscillating electric field in an incommensurate periodic "corrugation" potential of increasing magnitude U_0. We found the chain sliding to switch, as U_0 increases and before the Aubry transition, from a smooth-sliding regime with low dissipation to a stick-slip regime with high dissipation. In the stick-slip regime the onset of overall sliding is preceded by precursor events consisting of partial slips of a few ions only, leading to partial depinning of the chain, a nutshell remnant of precursor events at the onset of motion also observed in macroscopic sliders. Seeking to identify the possible effects on friction of a structural transition, we reduced the trapping potential aspect ratio until the ion chain shape turned from linear to zigzag. Dynamic friction was found to rise at the transition, reflecting the opening of other dissipation channels.

DOI: 10.1103/PhysRevB.87.195418 PACS number(s): 68.35.Af, 68.60.Bs, 64.70.Nd, 83.85.Vb

I. INTRODUCTION

Similarly to colloidal monolayers driven across laser-generated surfaces,[1,2] linear chains of cold ions trapped inside optical lattices have been recently proposed as novel candidates for studies in the field of friction.[3] One of the motivations has been the possibility to observe, thanks to their exceptional parameter tunability, the long theorized Aubry transition, namely, the switch between a regular frictional state and the "superlubric" state of vanishing static friction between idealized incommensurate one-dimensional (1D) "crystals." The key feature of friction between solid bodies is hysteresis, that is, the difference between to and fro motion. In time-periodic sliding motion, for example, hysteresis is responsible for the finite area enclosed by the force-displacement cycle, which exactly equals the frictional heat per cycle. Smallest when the sliding regime is smooth, friction turns large when sliding occurs by stick slip—a discontinuous stop and go which constitutes the largest and most common source of frictional hysteresis. Generally triggered by mechanical instabilities, stick slip takes place at geological, ordinary, and at nanometer length scales alike.[4–6] Restricting here to the nanoscale and microscale, which is the focus of much current work, we are naturally interested in microscopical systems exhibiting a controlled transition between smooth and stick-slip sliding regimes.

One-dimensional periodic ("crystalline") sliding models, although highly simplified, have long been used to illustrate frictional phenomena between periodic lattices.[7] In the so-called Frenkel-Kontorova (FK) model,[8] a harmonic chain of classical masses with average spacing a_o in a sinusoidal periodic potential of amplitude U_0 and wavelength λ (leading to a commensuration ratio $\eta = a_o/\lambda$ between the two) idealizes the sliding of two crystalline surfaces. Irrational values of η characterize the most interesting incommensurate case between slider and substrate. Aubry[9,10] proved long ago that a transition (where the ground state "hull function" exhibits analyticity breaking) occurs for increasing U_0, from what is now known as a *superlubric* state where the static friction F_S—the minimal force capable of initiating sliding—is exactly zero, to a *pinned* state where F_S is finite. While exceptionally low friction between incommensurate three-dimensional (3D) surfaces has indeed been observed experimentally,[11] experimental demonstrations of the Aubry transition in genuinely 1D systems are still lacking. Cold ion traps were recently invoked as possible candidates to display the Aubry transition, thereby surprisingly entering the field of nanotribology.[3] Although not identical to the FK model, the physics of repulsive 1D particles is expected to be essentially the same as each particle can still be seen as occupying the center of some overall harmonic potential. Experimentally,[12] chains of up to several tens of positive ions such as Ca^+ can be stabilized using rf quadrupolar fields and cooled down to temperatures below 1 μK. By tuning the confining cigar-shaped potential to a sufficiently elongated form, the ions can be forced to form linear chains. The periodic optical lattice potential for the ions is provided by a laser standing wave [see Fig. 1(a)].

The confined ion chains do constitute 1D crystal segments, but are not really homogeneous. The nearest-neighbor ion-ion distance, fairly constant at the center, increases at the periphery and diverges near the extremities, as shown in Fig. 1(b). Still, the chain center is a reasonable realization of an FK-like model, and some of the properties of an ideal infinite system can be in principle realized and observed there. When λ is incommensurate with respect to the central ion-ion spacing a_o, one can achieve, according to our recent predictions,[3] a strong and observable remnant of the Aubry transition also in such trapped ion chains. In the confined ion chain, the standard Aubry transition, which in the infinite chain occurs when the periodic potential ("corrugation") amplitude U_0 exceeds some critical threshold U_c, is replaced by a static, symmetry breaking transition of the ground state chain configuration and geometry. Benassi and co-workers[3] proposed to observe this transition by measuring the external uniform force F_R

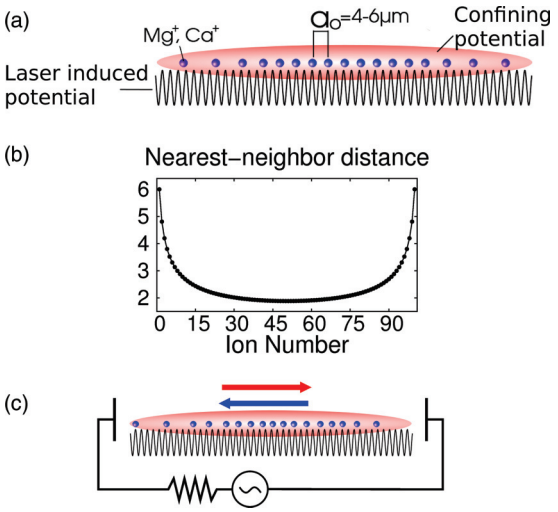

FIG. 1. (Color online) (a) Schematic of a linear ion chain trapped by an anisotropic confining potential. Typical ions used in experiments are Ca^+ or Mg^+, and the ion-ion distance at the center of the chain is of the order of few μm. (b) Nearest-neighbor distance (in dimensionless units, see Sec. II) between the ions of a 101-ion chain at rest and in the absence of the corrugation potential. (c) A possible experimental setup for the study of the dynamics of the chain using an external oscillating electric field.

needed to restore the symmetry. Simulations indeed showed that the effective static friction force F_R behaves and grows as a function of $U_0 > U_c$ very closely as the static friction force F_S of the ideal infinite chain, thus demonstrating the connection between the two [see Fig. 2].

In this paper we move from static friction to the dynamical sliding properties of the ion chain, once depinned by an additional external electric field, as a function of the periodic corrugation amplitude U_0 [see Fig. 1(c)]. We show that the trapped cold ions can slide either smoothly or by stick slip, with a parameter-controlled transition and a correspondingly strong frictional rise between the former and the latter. Drawing an analogy with macroscopic frictional experiments, the corrugation U_0 plays here the role of the load in ordinary sliding

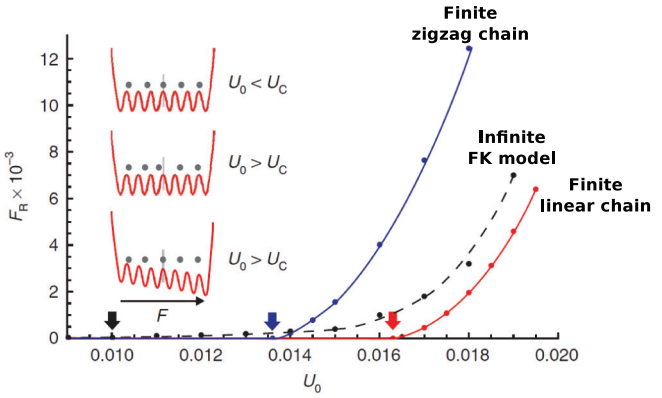

FIG. 2. (Color online) Effective static friction of a 101-ion chain in the linear (red) and zigzag (blue) configuration plotted against the corrugation potential amplitude U_0. The black dashed line is the static friction of the ideal FK model. The arrows indicate the values of U_0 at which F_R vanishes. (From Ref. 3.)

friction. As expected, we find and characterize the transition from a poorly dissipative smooth-sliding regime to a highly dissipative stick-slip regime as U_0 is increased. Moreover, since the cold ion ground state geometric configuration can be pushed across parameter-driven structural transitions by changing the trapping potential conditions, we investigate the effect of a phase transition on sliding friction, which is of interest as well.[13] As is known both theoretically[14,15] and experimentally,[16] a change of aspect ratio in the confining trap effective potential causes the ion chain to cross a series of structural transitions. If and when for a sufficiently long chain these transitions can be considered continuous, the friction behavior near the transition point could show remnants of the chain's critical behavior, as recently suggested theoretically.[13]

In anticipation of future experiments, we carried out classical molecular dynamics simulations of a 101-ion chain sliding in a golden ratio incommensurate corrugated potential, with a view to predict and discuss the basic dynamic frictional phenomena of an electric field solicited trapped ion chain. In Sec. II we will describe the model and the protocol used for the molecular dynamics (MD) simulations. Section III will be devoted to the resulting smooth to stick-slip frictional switch and the observation of precursor events at the onset of the chain sliding. In Sec. IV we describe the change of the frictional behavior across the linear-zigzag structural transition. Finally, Sec. V contains our discussion and conclusions.

II. TRAPPED ION CHAIN MODEL AND SLIDING SIMULATION PROTOCOL

The effective potential of an ion of charge q in a linear anisotropic (Paul) trap can be written as[17]

$$V_{\text{eff}}(x,y,z) = \frac{1}{2m}[\omega_\perp^2(x^2+y^2)+\omega_\parallel^2 z^2], \tag{1}$$

where m is the mass of the ion and $\omega_\perp^2$ and $\omega_\parallel^2$ are the strengths of the confining effective potential, supposed to be harmonic, in the transverse and longitudinal directions. In order to work in dimensionless units we define the length unit d:

$$d = \left(\frac{q^2}{4\pi\epsilon_0 m\omega_\perp^2}\right)^{1/3}. \tag{2}$$

We then measure masses in units of m, charges in units of q, energy in units of $q^2/(4\pi\epsilon_0 d)$, forces in units of $q^2/(4\pi\epsilon_0 d^2)$, and time in units of $1/\omega_\perp$. The effective Hamiltonian of N trapped ions is then[18,19]

$$H_{\text{eff}} = \sum_{i=1}^{N}\left\{\frac{\mathbf{p}_i^2}{2}+\frac{1}{2}\left[\omega_\perp^2\left(x_i^2+y_i^2\right)+\omega_\parallel^2 z_i^2\right] + U_0\cos\left(\frac{2\pi}{\lambda}z_i\right)+\sum_{j\neq i}\frac{1}{|\mathbf{r}_i-\mathbf{r}_j|}\right\}, \tag{3}$$

where the sinusoidal term represents a laser induced periodic potential, mimicking the corrugation of a hypothetical crystalline substrate lattice.

The ground state geometry of the ions at $T=0$ depends on the aspect ratio $R=(\omega_\parallel/\omega_\perp)^2$ of the anisotropic harmonic confining potential. For small enough R the potential is

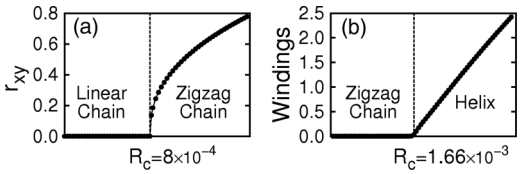

FIG. 3. (a) Linear-zigzag structural transition of a 101-ion chain. r_{xy} is the maximum displacement of the ions from the z axis. (b) Zigzag-helix transition. The order parameter is the number of windings of the ions around the z axis.

cigarlike, and ions form a linear chain along the trap symmetry axis z. As R is increased, there is a sequence of shape transitions: first, from a straight chain to a planar zigzag chain, and next, a second transition where planarity is lost, and the planar zigzag turns into a helix. Still at $T = 0$, and for an infinite chain, both classical transitions are continuous,[20] as shown in Fig. 3.

We simulated, following Benassi *et al.*,[3] a chain of 101 positive ions choosing $\omega_\parallel^2 = 0.0005$, $R = 0.0005$, and $\eta = \lambda/a_o = 2/(1+\sqrt{5})$, where a_o is the center ion-ion spacing. Chain sliding is caused by an external slowly oscillating electric field $\mathbf{E}(t) = \hat{\mathbf{z}} E_0 \sin(\Omega t)$ acting on each ion in the longitudinal direction z. We carried out classical damped molecular dynamics (MD) integrating the equations of motion using a standard velocity-Verlet algorithm with time step $\Delta t = 0.005$. At each time the total force acting on the ith ion is given by

$$\ddot{\mathbf{r}}_i = \mathbf{F}_i^{\text{Coul}} + \mathbf{F}_i^{\text{trap}} + \mathbf{F}_i^{\text{sub}} - \gamma \mathbf{v}_i, \tag{4}$$

where we have, respectively, the force due to the ion-ion Coulomb repulsion, the confining potential force, the corrugation force, and a velocity dependent dissipative force controlled by a damping parameter γ. There is no random force, corresponding to our $T = 0$ background assumption. The trap confinement plus oscillating potential is given by

$$V_{\text{ext}}(z) = \frac{\omega_\parallel^2}{2} z^2 - z E_0 \sin(\Omega t), \tag{5}$$

which is a confining parabola of vertex $z_{\text{trap}} = E_0 \sin(\Omega t)/\omega_\parallel^2$ moving at velocity $v_{\text{trap}} = E_0 \Omega \cos(\Omega t)/\omega_\parallel^2$. In order to follow stick slip, when present, we monitored the distance of the center of mass of the chain from the minimum of the moving parabola:

$$\delta z_{\text{cm}}(t) = z_{\text{trap}}(t) - z_{\text{cm}}(t). \tag{6}$$

Figure 4 shows an example of the time evolution of δz_{cm} corresponding to a sequence of external electric field oscillations. The dynamic friction of the system is computed as the work W done by the oscillating electric field on all the particles:

$$W_k = \frac{1}{N} \sum_{i=1}^{N} \int_k dt [\mathbf{v}_i \cdot \hat{\mathbf{z}} E_0 \sin(\Omega t)], \tag{7}$$

where the integral is calculated over the kth period corresponding to the electric field going from its minimum value $-E_0$ to its maximum value $+E_0$ and back. The final estimate of the dynamic friction is obtained from the average of the M samples W_k measured during the whole trajectory: $W = \frac{1}{M} \sum_{k=1}^{M} W_k$.

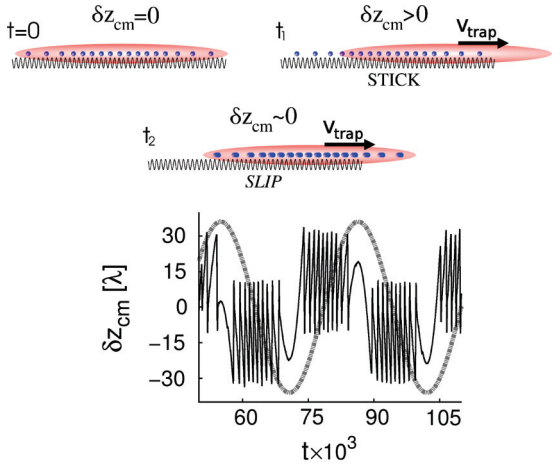

FIG. 4. (Color online) Dynamics of δz_{cm} (see text) under periodic sliding. At $t = 0$ the chain is almost symmetric with respect to the vertex of the confining parabola and $\delta z_{\text{cm}} \approx 0$; if the chain is locked to the substrate, δz_{cm} increases as the confining potential moves until a slip event occurs, which corresponds to a sudden drop to zero of δz_{cm}. The plot shows a result from a simulation where many slip events are observed during each oscillation back and forth of the chain over the substrate. The gray dashed line corresponds to the external electric field.

III. RESULTS: DYNAMIC FRICTION, STICK-SLIP, AND PRECURSOR EVENTS

Figure 5(a) shows the frictional work W done by the external electric field on the trapped ion chain as a function of the corrugation amplitude U_0. The inset depicts schematically the expected behavior in the infinite incommensurate FK model, where for $U_0 < U_c$, below the Aubry transition,

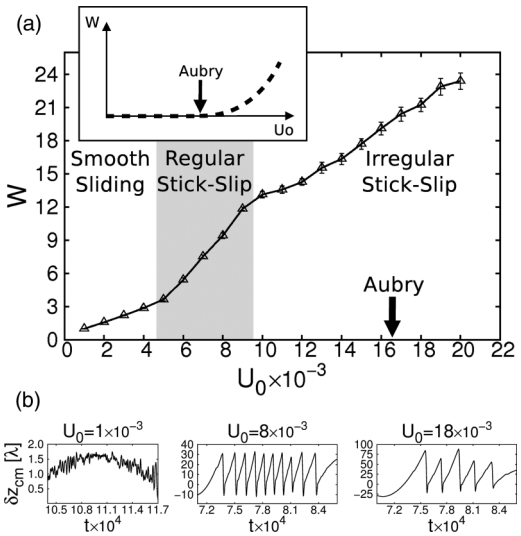

FIG. 5. (a) Dynamic friction W of the oscillating ion chain as a function of the corrugation amplitude U_0. The values of $E_0 = 0.1625$, $\Omega = 0.0002$, $\gamma = 0.01$ were chosen so as to yield 4–5 slip events during each oscillation, in correspondence to the highest values of U_0 investigated. (b) Dynamics of δz_{cm} in the three different regimes of smooth sliding, regular, and irregular stick slip. The time interval plotted corresponds approximately to half a period of the oscillating electric field which increases from $-E_0$ to $+E_0$.

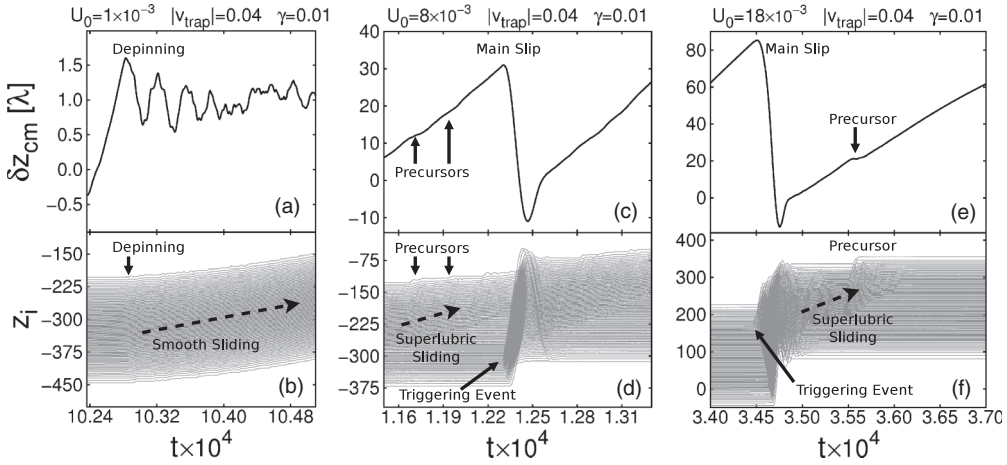

FIG. 6. (a) Dynamics of $\delta z_{\rm cm}$ in the smooth-sliding regime; (b) shows the corresponding trajectories of each ion. (c) Dynamics of $\delta z_{\rm cm}$ in the regular stick-slip regime; (d) shows the corresponding trajectories of each ion. (e) Dynamics of $\delta z_{\rm cm}$ in the irregular stick-slip regime; (f) shows the corresponding trajectories of each ion. The features highlighted in the figure are discussed in Sec. III.

motion takes place without static friction, and kinetic friction vanishes in the limit of infinitely slow sliding. In the chain of trapped ions, finite and inhomogeneous, the static friction force needed for overall chain motion is nonzero for all corrugations, since the two extremities are always locked to the corrugation potential. Correspondingly, there is upon sliding a finite frictional dissipation W for all values of U_0. For the chosen external field frequency $\Omega = 0.0002$ and amplitude $E_0 = 0.1625$ friction grows steadily with corrugation U_0 and nothing significant happens to the dynamic friction W across the nominal[3] Aubry value $U_c = 0.016\,28$. In fact, the dynamics of the chain does not change appreciably above $U_0 \approx 0.01$.

We can resolve, based on the detailed nature of the sliding trajectories, three different dynamical regimes. Figure 5(b) shows the dynamics of $\delta z_{\rm cm}$ for three representative values of U_0. For small corrugations $U_0 \leqslant U_{01} = 0.005$ the chain follows smoothly the external force and the friction is modest (with a value determined by, and growing with, the sliding velocity, in turn proportional to Ω). As U_0 is increased further, the smooth-sliding dynamics is replaced by a regular, time-periodic stick-slip regime with an accompanying increase of dissipation. As long as $U_{01} \leqslant U_0 \leqslant U_{02} = 0.01$ the slip magnitude is fairly constant during each oscillation. For larger corrugations finally, $U_0 \geqslant U_{02}$ the chain enters a chaotic regime of irregular stick slip.

Figure 6 shows details of the trajectories of the chain center of mass and of all individual ions in the three regimes. For $U_0 \leqslant U_{01}$ the chain is weakly pinned at the inversions of motion occurring for $E(t) = \pm E_0$. After the depinning the chain follows smoothly the external force; small oscillations of $\delta z_{\rm cm}$ are due to the internal motion of the chain [see Figs. 6(a) and 6(b)]. A number of interesting features appear at the onset of stick-slip $U_0 \geqslant U_{01}$ and they are shown in Figs. 6(c)–6(f). The head and the tail of the ion crystal are locked to the corrugation potential [see the top and bottom parts of Fig. 6(d), initial times] while the truly incommensurate central part is free to slide, thus increasing the ion density of the head, reducing that of the tail and inducing partial depinnings of the chain. The precursor events appear in the head part [see the top part of Fig. 6(d), times between $t = 1.16$ and $t = 1.22$]. Although different and connected with inhomogeneity of stress rather than of contact, partial precursors were also shown to precede the onset of macroscopic sliding by Fineberg's group.[21,22] Partial slips of the chain always start within the central superlubric region and proceed moving in the direction of the external force. They are present only in the stick-slip regime and disappear by increasing the average pulling velocity $|v_{\rm trap}| = 2E_0\Omega/\pi\omega_\parallel^2$ of the trapping potential [see Fig. 7]. Following the precursors, as stress accumulates more and more in time, the system undergoes a mechanical instability

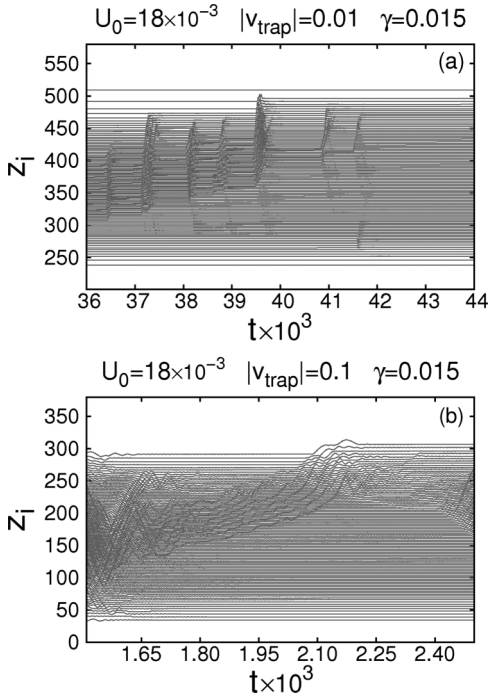

FIG. 7. Precursor events observed between two main slip events for (a) $|v_{\rm trap}| = 10^{-2}$ and (b) $|v_{\rm trap}| = 10^{-1}$. As the pulling velocity is increased, the precursor events disappear, signaling the transition from stick-slip motion to smooth sliding.

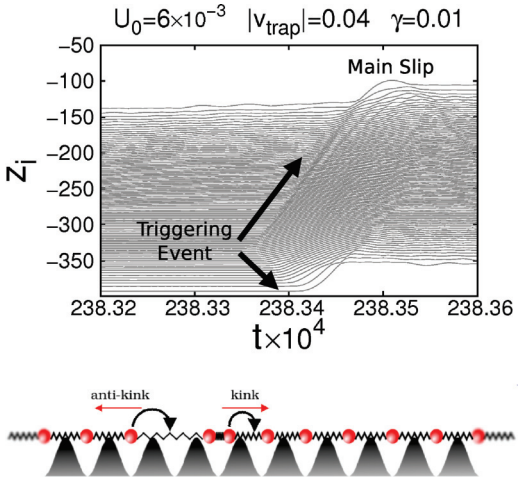

FIG. 8. (Color online) Example of a triggering event inducing the main slip.

typical of stick slip.[6] The ensuing main slip of the whole system is triggered by the creation of a kink-antikink pair (see Fig. 8). In the regular stick-slip regime $U_{01} \leqslant U_0 \leqslant U_{02}$ the tail drives the sliding onset, and the triggering pair forms in the tail region, while the chain center and front are still free to slide [see Fig. 6(d), times between $t = 1.22$ and $t = 1.25$]. In the chaotic stick-slip regime $U_0 \geqslant U_{02}$ instead, the onset of sliding is different. The central superlubric flow and partial slips of the front ions first bring the chain into a metastable state where each ion is locked to the corrugation [see Fig. 6(f), times between $t = 3.5$ and $t = 3.6$]. The generation of a kink-antikink pair forming now in the chain head, as opposed to the chain tail of the previous regime, eventually leads to global sliding, as shown by the main slip event at the initial times of Fig. 6(f). This tail-to-head switch of the triggering event is a characteristic signature always accompanying the passage from regular to chaotic stick slip. On the other hand, neither the sliding onset dynamics nor the dynamical friction magnitude finally display any particular feature or singularity when the corrugation grows across the Aubry transition. This result underlines a substantial difference between the frictional behavior of this short and inhomogeneous chain, and that expected of an ideally infinite and uniform FK-like chain. In the latter and ideal system there is no other transition than Aubry, and in the limit of zero sliding speed stick-slip sliding can only take place when static friction turns nonzero, which is above the Aubry transition. Figure 9 shows details of the sliding dynamics in the strongly corrugated, chaotic stick-slip regime. The average nearest-neighbor distance between the central 31-ion portion is displayed as a function of time between two main slips of the crystal. The initial passage of the "superlubric" front brings the central part to a commensurate configuration with ions spaced exactly by 2λ (instead of the original golden ratio spacing 1.618λ) from one another. This dynamically induced commensuration brings the whole chain to a temporarily locked state, thus increasing the static friction force needed for the onset of overall motion.[23] Subsequent depinning of the chain off this locked state only occurs as the external force grows further, and is sudden. This two-stage nature of sliding, and the relative abruptness of the depinning, is at the origin of the chaotic behavior of stick slip in this regime.

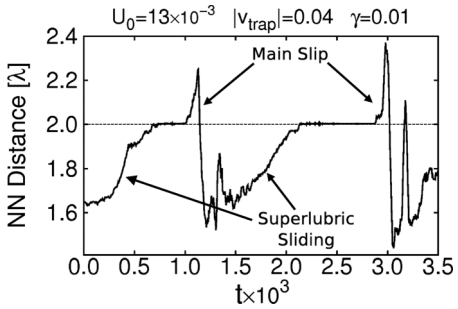

FIG. 9. Average ion-ion distance (in units of λ) vs time; we considered only the central 31 ions of the chain. After the passage of the superlubric front, the center of the chain is left in a commensurate configuration with ions equally spaced by 2λ. The same kind of dynamics occurs at the onset of motion at each values of U_0 in the stick-slip region.

IV. FRICTION SINGULARITY AT THE LINEAR-ZIGZAG STRUCTURAL TRANSITION

Benassi *et al.* recently proposed that interesting frictional changes or anomalies could be observed in the presence of structural phase transitions.[13] Although a 101-ion chain is a long way away from an infinite system, it is still interesting to find out what singularities would friction develop upon an overall, collective shape change. To study that, we carried out simulations at values of the trapping potential aspect ratio R straddling the critical value $R_c = 0.0008$ for the linear-zigzag transition. Although this kind of effect should be quite general, the expected delicacy of this frictional feature should best become apparent under sliding conditions with limited noise, such as those expected at weak corrugations. Setting $U_0 = 0.0008$ and also γ, Ω, and E_0 values which lead to a smooth and gentle sliding dynamics (disturbing the chain to a minimal extent) we obtained the dynamic friction of Fig. 10(a). Deep enough in the linear chain regime ($R \leqslant 0.000\,64$) the ions remain in a strictly 1D configuration during the whole dynamics. Here, only longitudinal internal vibration degrees of freedom of the chain are excited and W is small and essentially independent of R. As the critical anisotropy R_c is approached, the transverse vibration modes of the chain soften and become rather suddenly excitable, a different dissipative channel opens, and W rises, anticipating the linear-zigzag transition. In a hypothetical infinite chain, where the transition occurs continuously and critically, the frictional behavior will presumably also exhibit a critical singularity. Given the finite chain size, the frictional rise is smooth, although it can still be sharpened by reducing the corrugation amplitude. Figures 10(b) and 10(c) show results of simulations with U_0 reduced down to 0.0004, 0.0001, and a lower value of E_0. The transverse mode excitation onset occurs nearer to R_c.

That result is made clearer in Fig. 10(d), where the standard deviation $\sigma_{r_{xy}}$ of the maximum displacement of the ions away from the z axis is plotted against the aspect ratio R. Denoting with $\langle \cdots \rangle$ the time average over the whole trajectory, $\sigma_{r_{xy}}$ and

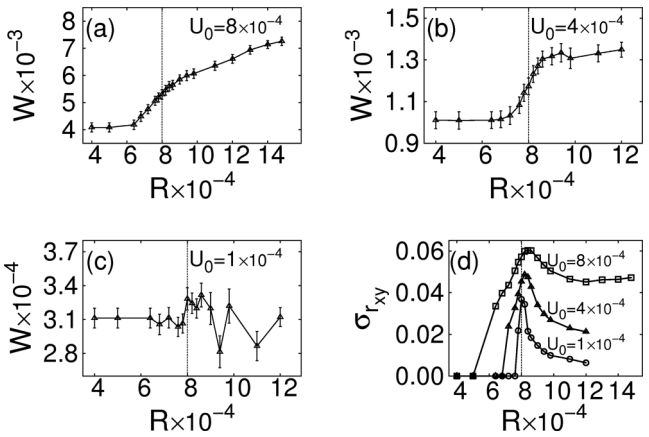

FIG. 10. (a) Dynamic friction across the linear-zigzag transition for $U_0 = 0.0008$. The parameters used are $\gamma = 0.0005$, $E_0 = 0.005\,078\,125$, $\Omega = 0.0032$. Without a corrugation potential the chain moves as a rigid body at a very low dissipation rate independent on R (not shown). As U_0 is switched on, the internal degrees of freedom of the chain begin to dissipate. In this set of simulations the transverse modes begin to be excited at $R \approx 0.000\,64$. (b) Dynamic friction across the linear-zigzag transition for $U_0 = 0.0004$ and (c) $U_0 = 0.0001$, using $E_0 = 0.002\,539\,063$, $\Omega = 0.0032$, $\gamma = 0.0005$. By lowering the external electric field and the amplitude of the substrate potential, the onset of the excitation of the transverse modes is shifted towards the static critical value $R_c = 0.0008$. In this set of simulations the transverse modes begin to be excited at $R \approx 0.000\,72$ and $R \approx 0.000\,78$, respectively, for $U_0 = 0.0004$ and $U_0 = 0.0001$. (d) Standard deviation $\sigma_{r_{xy}}$ of the maximum displacement r_{xy} of the ions from the z axis plotted as a function of R and measured using the whole trajectories of the simulations of (a)–(c). $\sigma_{r_{xy}}$ is zero until the transverse modes begin to be excited and it shows a clear maximum near R_c, which becomes sharper as U_0 is decreased.

r_{xy} are defined as

$$\sigma_{r_{xy}} = \sqrt{\langle (r_{xy} - \langle r_{xy} \rangle)^2 \rangle}, \tag{8}$$

$$r_{xy} = \mathrm{Max}_{\{i=1,N_{\mathrm{ions}}\}} \left(\sqrt{x_i^2 + y_i^2} \right). \tag{9}$$

$\sigma_{r_{xy}}$ is zero until the transverse modes begin to be excited and it displays a maximum near the critical point R_c.

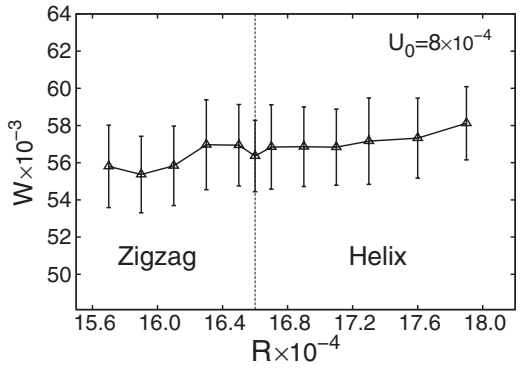

FIG. 11. Dynamic friction across the zigzag-helix transition. The dissipative properties of the chain are not affected by the helical distortion. The parameters used are $\gamma = 0.0005$, $E_0 = 0.040\,625$, $\Omega = 0.0004$, $U_0 = 0.0008$.

A further increase of R drives a subsequent transition of the trapped ion geometry from zigzag to helix. Figure 11 shows the behavior which we obtained for the dynamic friction across this transition. Not much happens here. In this case, in fact, on both sides of the critical point the chain is already in a 3D configuration and its dissipative properties are not significantly affected by the weaker helical distortion.

V. CONCLUSIONS

By means of classical damped MD we simulated a 101-ion linear chain executing a forced time-periodic sliding over a (laser induced) space-periodic "corrugation" potential of strength U_0 whose wavelength λ was golden mean incommensurate with respect to the center ion-ion spacing. As U_0 was increased, the system turned from smooth-sliding to a stick-slip sliding regime, first regular and then chaotic. We observed as expected an increase in the dissipation rate at the onset of stick slip, as is also observed in macroscopic dry friction when the loading force is increased.

Three separate frictional regimes were identified, as a function of corrugation amplitude. A smooth-sliding one for weak corrugation was followed by time-periodic stick-slip sliding at larger corrugation, eventually leading to chaotic stick slip for even larger corrugation.

Due to the inhomogeneity of the ion crystal, the frictional dynamics of the ion chain showed several different features reflected in the ion trajectories. The two chain extremities were always pinned while the incommensurate central part was free to slide following the external force. The onset of motion in the stick-slip regime was characterized by the presence of precursor events, i.e., partial slips of side chain portions induced by the superlubric flow of the truly incommensurate central part.

The chaotic stick slip at large corrugation was connected by an interesting two-stage process. First, superlubric sliding of the central portion brought the chain to a temporary commensurate state, locked to the periodic corrugation. Subsequently, as force grew, a kink-antikink pair was generated and propagated toward the extremities, eventually inducing the slip of the whole system.

We also studied the possible anomalies of friction dissipation across the structural phase transformations of the trapped ions obtained by varying the aspect ratio $R = (\omega_\parallel/\omega_\perp)^2$ of the harmonic trapping potential. At fixed $\omega_\parallel$, as R was increased, the ion chain transformed first from a linear configuration to a planar zigzag and then to a helix. The energy dissipation increased characteristically at the linear to zigzag transition. Conversely, the zigzag to helix transition did not yield significant frictional changes.

Considerations about experimentally accessible system parameters, which are given in the Appendix, suggest that some of these features, if not all, should become observable in future experiments with Ca^+ ion traps.

ACKNOWLEDGMENTS

This work was partly sponsored by Contracts PRIN/COFIN 2010LLKJBX_004, Sinergia CRSII2$_1$36287/1, and by advances of ERC Advanced Grant No. 320796–MODPHYSFRICT. Discussions with A. Benassi, T. Pruttivarasin, and H. Häffner are gratefully acknowledged.

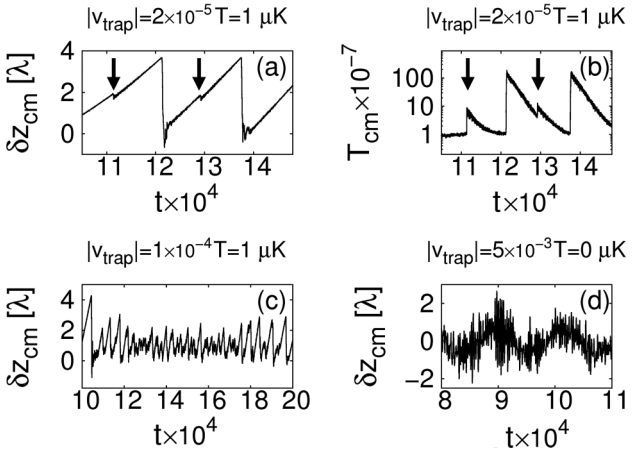

FIG. 12. 101-ion chain. (a) $\delta z_{\rm cm}$ in the simulation at $|v_{\rm trap}| = 2 \times 10^{-5}$ and $T = 10^{-7}$ showing stick-slip and precursor events (indicated by the arrows) corresponding to partial slips of the central portion of the chain. (b) Temperature measured in the center of mass frame in the simulation of (a). After each slip event the internal temperature is raised and then it is exponentially damped by the thermostat. Precursor events give rise to the smaller peaks, indicated by the arrows. This trend is always observed in the stick-slip regime. (c) For $|v_{\rm trap}| = 10^{-4}$ and $T = 10^{-7}$ the dynamics is chaotic. Slips of different magnitude occur as the pulling velocity changes during each oscillation. (d) Further increasing $|v_{\rm trap}| = 5 \times 10^{-3}$ the dynamics finally turns into a smooth-sliding regime, even at $T = 0$.

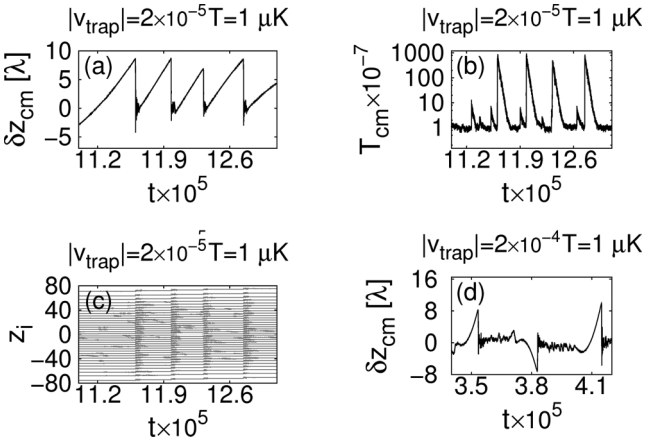

FIG. 13. 35-ion chain. (a) $\delta z_{\rm cm}$ in the simulation at $|v_{\rm trap}| = 2 \times 10^{-5}$ and $T = 10^{-7}$. An irregular stick-slip regime is observed. (b) Temperature measured in the center of mass frame in the simulation of (a). The highest peaks correspond to the main slip events, with slips of a few ions within the chain giving rise to the smaller ones. (c) Trajectory of each ion during some slip events of the simulation of (a) and (b). The chain slip as a whole and precursor events are not observed due to the small size of the system. (d) $\delta z_{\rm cm}$ in the simulation at $|v_{\rm trap}| = 2 \times 10^{-4}$ and $T = 10^{-7}$. At the inversions of motion the chain is pinned; owing to the small initial pulling velocity, a sharp slip event occurs after which smooth sliding begins.

APPENDIX: PRACTICAL PARAMETER CHOICES

In order to create an optical lattice, the laser wavelength must fit one of the electronic transitions of the chosen ions. For Ca^+ the $S_{1/2}$-$P_{1/2}$ transition at 397 nm is naturally exploited, leading to a lattice spacing $\lambda \approx 200$ nm. An achievable amplitude for the corrugation potential is of the order of 10^{-27} J. If we consider a transverse trapping frequency $\omega_\perp = 2\pi \times 4$ MHz, we get (in dimensionless units) $\lambda = 0.115$, $U_0 = 2.31 \times 10^{-5}$. A practically achieved temperature is $T = 10^{-7}$, corresponding to 1 μK. Setting an aspect ratio $R = 0.0005$, we have $a_o \approx 16\lambda$, therefore ions are separated by several lattice spacings, corresponding to a much "weaker" kind of incommensurability than the golden ratio used in the study so far. Moreover, for such a small value of U_0, the chain is almost free to slide, in this case also the two extremities being weakly anchored to the substrate. Stick slip is therefore expected to occur only at very small pulling velocities when, after each slip, the chain is allowed to relax in a different metastable pinned configuration. We performed simulations at the experimental parameters for the 101-ion and a 35-ion chain using the same protocol described above. We chose $\gamma = 0.0005$ and we used a Langevin thermostat for the simulations at finite T. We also set Ω and E_0 in order to test different average velocities of the moving confining parabola.

Let us consider first the 101-ion chain. At very low pulling velocity we observed stick-slip motion, the slip amplitude being of the order of a few lattice parameters [see Fig. 12(a)]. The dynamics of the slip events is simple and no longer shows the variety of features described previously for the golden ratio incommensurability. The pinned chain remained stable upon pulling until a weak compression generated within the chain propagates toward the head. Simple precursor events are observed consisting of partial slips of a central portion of the chain at fixed extremities (not shown). Figure 12(b) shows the temperature $T_{\rm cm}$ measured in the center of mass frame, displaying the expected inverse sawtooth behavior when plotted in a semilogarithmic scale. After each slip $T_{\rm cm}$ increases, and is then exponentially damped by the thermostat. As the pulling velocity is increased, the dynamics turns gradually into a smooth-sliding regime, as shown in Figs. 12(c) and 12(d).

Chains of a few tens of ions may be more easily stabilized inside a trap. We performed simulations with a 35-ion chain, using the same parameters as above. In this case the central ion-ion spacing is larger and corresponds to $a_o \approx 30\lambda$. As shown in Fig. 13(a), we observed that stick-slip motion is again preserved in this case as well as for small enough average pulling velocities. The slip amplitude is larger than that observed for the 101-ion chain, indicating a stronger pinning to the substrate, as is reasonable to expect given a larger prevalence of extremities. From the plot of the temperature of Fig. 13(b) we see that small adjustments of the inner ions occur, which give rise to small peaks in $T_{\rm cm}$, however, without proper precursor events due to the reduced size of the chain.

[1]T. Bohlein, J. Mikheal, and C. Bechinger, Nat. Mater. **11**, 126 (2011).

[2]A. Vanossi, N. Manini, and E. Tosatti, Proc. Natl. Acad. Sci. USA **109**, 16429 (2012).

[3]A. Benassi, A. Vanossi, and E. Tosatti, Nat. Commun. **2**, 236 (2011).
[4]F. B. Bowden and D. Tabor, *The Friction and Lubrication of Solids* (Oxford University Press, New York, 1950).
[5]B. N. J. Persson, *Sliding Friction* (Springer, Berlin, 1998).
[6]A. Vanossi, N. Manini, M. Urbakh, S. Zapperi, and E. Tosatti, Rev. Mod. Phys. **85**, 529 (2013).
[7]A. Vanossi and O. M. Braun, J. Phys.: Condens. Matter **19**, 305017 (2007).
[8]O. M. Braun and Y. Kivshar, *The Frenkel-Kontorova Model: Concepts, Methods, and Applications* (Springer, Berlin, 1998).
[9]S. Aubry and P. Y. Le Daeron, Physica D **8**, 381 (1983).
[10]M. Peyrard and S. Aubry, J. Phys. C: Solid State Phys. **16**, 1593 (1983).
[11]M. Dienwiebel, G. S. Verhoeven, N. Pradeep, J. W. M. Frenken, J. A. Heimberg, and H. W. Zandbergen, Phys. Rev. Lett. **92**, 126101 (2004).
[12]T. Pruttivarasin, M. Ramm, I. Talukdar, A. Kreuter, and H. Häffner, New J. Phys. **13**, 075012 (2011).
[13]A. Benassi, A. Vanossi, G. E. Santoro, and E. Tosatti, Phys. Rev. Lett. **106**, 256102 (2011).
[14]J. P. Schiffer, Phys. Rev. Lett. **70**, 818 (1993).
[15]S. Fishman, G. De Chiara, T. Calarco, and G. Morigi, Phys. Rev. B **77**, 064111 (2008).
[16]M. G. Raizen, J. M. Gilligan, J. C. Bergquist, W. M. Itano, and D. J. Wineland, Phys. Rev. A **45**, 6493 (1992).
[17]F. G. Major, V. N. Gheorghe, and G. Werthe, *Charged Particle Traps* (Springer, Berlin, 2005).
[18]G. Morigi and S. Fishman, Phys. Rev. Lett. **93**, 170602 (2004).
[19]G. Morigi and S. Fishman, Phys. Rev. E **70**, 066141 (2004).
[20]Note that, strictly speaking, at $T = 0$ we should not ignore quantum effects and treat this transition as a quantum critical point, as developed, for example, in Ref. 24.
[21]S. M. Rubinstein, G. Cohen, and J. Fineberg, Nature (London) **430**, 1005 (2004).
[22]S. M. Rubinstein, G. Cohen, and J. Fineberg, Phys. Rev. Lett. **98**, 226103 (2007).
[23]A similar behavior has been observed in MD simulations of 2D mesoscopic colloidal monolayers driven over an incommensurate optical lattice (Ref. 2).
[24]E. Shimshoni, G. Morigi, and S. Fishman, Phys. Rev. A **83**, 032308 (2011).